Desalination and Water Treatment
www.deswater.com

doi: 10.5004/dwt.2023.29697

299 (2023) 118–127
July

Removal of chromium(III) ion from tannery wastewater and river water using natural and activated orange peel

Ishtiaq Ahmed Jawad[a], Adib H. Chisty[a,*], Mohammed Mizanur Rahman[b]

[a]*Institute of Leather Engineering and Technology, University of Dhaka, Dhaka, Bangladesh, Phone: +880-1917033843; email: adibchisty@du.ac.bd (A.H. Chisty)*
[b]*Department of Applied Chemistry and Chemical Engineering, University of Dhaka, Dhaka, Bangladesh*

Received 13 November 2022; Accepted 5 June 2023

ABSTRACT

In this study, the adsorption method was used to explore the removal of chromium(III) ion from chrome liquor that remained after chrome tanning in tannery and from the Buriganga River water as well. Both the natural and activated orange peel powder were used as adsorbents owing to its inexpensive and eco-friendly nature. In order to establish the best adsorption conditions, adsorbent concentration 5–40 g/L, pH 2–8 and contact time 30–120 min were investigated for Cr(III) removal from aqueous solutions using both natural orange peel and activated orange peel. Characterization of the adsorbents were done by using thermogravimetric analysis and Fourier-transform infrared spectroscopy analysis. The equations for both the Langmuir and Freundlich models were implemented to analyze the equilibrium data. Furthermore, the pseudo-first and second-order kinetic models were also utilized to evaluate the kinetic data. Both the natural and activated orange peel were found to remove a maximum of 77% and 96% of chromium(III) ion, respectively.

Keywords: Adsorption; Chromium(III); Orange peel; Activated carbon

1. Introduction

In this current era, the generation of chromium during the tanning process of leather is one of the major environmental issues around the world. Every day, a significant amount of tannery effluent including heavy metals (of which chromium is a crucial component) is released into waterbodies [1]. Chrome(III) and chrome(VI) are the two states of chrome that can be found in nature. Chemical, epidemiological, and toxicological characteristics of chromium(III) and chromium(VI) are dissimilar. Although plants do not need the chromium(III), it is essential for humans and other animals in the lipid and sugar metabolism process. However, living things suffer severe health issues when they absorb more chromium than necessary. Therefore, determining the quantity of chromium and removing it from any components is a crucial task [2]. Chromium contamination is a serious danger to the ecosystem and has a negative effect on our environment and natural resources, particularly water and soil. Increased levels of accumulation in human and animal tissues due to excessive exposure of chromium might have toxic and harmful health consequences. In addition, the development of the leather industry in Bangladesh requires a decrease in chromium generation. No industry will be able to obtain an LWG certification without lowering environmental pollutants. European nations will not buy leather from any nation without the LWG certification. Additionally, the main rivers in Bangladesh are being contaminated by this pollution. Previously, the river Buriganga, located in Dhaka, was being polluted by the tannery industry. Due to the relocation of the industry to Savar, it is now contaminating Shitalakkha. In Savar, CETP is not functioning well. Therefore, a suitable approach must be needed to reduce the pollution brought on by chromium [3].

Numerous studies have been conducted to find ways to keep harmful and heavy materials including copper,

* Corresponding author.

lead, cerium, and vanadium from contaminating the ecosystem [4–14]. Additionally, a lot of work has been done to lessen the amount of chromium that enters the environment [15,16]. Moreover, many methods have been developed in the past years to reduce the amount of chromium(III) entering into the environment, like reduction and precipitation [17], ion exchange [18–20], adsorption [21], reverse osmosis [22], ultrafiltration [23,24], electrodialysis [25,26] and many more [27]. But these methods have some drawbacks like the fact that some of them are expensive, some are not feasible in every location, some are not easily accessible and various other reasons.

Utilizing an adsorbent to remove chrome(III) from chrome liquor used in leather tanning might be a game-changing move for the leather industry worldwide. Adsorption is known as the separation of a substance from one phase and the subsequent accumulation or concentration of that substance on the surface of another. Adsorbate refers to the material condensed or adsorbed on the surface of an adsorbent, which is the adsorbing phase. Adsorption is distinct from absorption, which takes place when substance is transferred through one phase to another (for instance, a liquid) and enters the second phase to create a "solution". Both processes are referred to under the umbrella term "sorption". An appropriate, cost-efficient, green, and highly effective adsorbent need to be developed [28]. Many items and wastes that are produced over the course of our daily lives, such as cotton balls, orange, onion, and banana peels, wood, wax paper, paper towels, and sandwich wrap, can be utilized as adsorbents. Orange peel adsorbent can be an excellent alternative to reduce the amount of chromium entering into the environment as it is a suitable, affordable, environment friendly and high effective process.

In this work, a simple procedure and easily accessible equipment are used to remove chromium(III) from tannery waste water and river water using natural orange peel and activated orange peel. To activate orange peel potassium hydroxide (KOH) was used.

2. Materials and methods

2.1. Materials

Potassium hydroxide (KOH), sodium hydroxide (NaOH), hydrochloric acid (HCl) and distilled water were used in this study. Every chemical was of the analytical reagent quality.

2.2. Preparation of adsorbent

2.2.1. Natural orange peel powder

At first, the orange peel was collected from oranges which were cultivated in Bangladesh. Then, the orange peels were washed four times by water to remove water soluble pollutants. After the orange peel got cleaned, it was dried in an oven at 110°C. Drying was done to reduce the moisture content of the orange peel. After 4 h of drying, the orange peel was taken off from the oven. After that, the dried samples are subsequently crushed to get the powdered sample. Then the powder was kept in an airtight container for further processes so that it doesn't come in contact with air. This powder was used as natural orange peel adsorbent.

2.2.2. Activated orange peel powder

40 g of orange peel powder was taken in a porcelain bowl for pre-carbonization process. Then the powder containing bowl was kept at furnace at 150°C for 1 h. After 1 h pre-carbonization process was done and the bowl was taken out from the furnace.

Due to the intercalation of metallic potassium, the KOH activation process is well recognized for creating pores on the carbon. In general, the KOH activation of carbon is a complex process. Several theories have been put up in the literature, but the real mechanism is complex and not fully understood. According to literature accounts, the following equations have been used to explain how the KOH activation process creates porous networks.

$$6KOH + 2C \rightarrow 2K + 3H_2 + 2K_2CO_3 \quad \text{(I)}$$

$$K_2CO_3 \rightarrow K_2O + CO_2 \quad \text{(II)}$$

$$K_2CO_3 + 2C \rightarrow 2K + 3CO \quad \text{(III)}$$

$$CO_2 + C \rightarrow 2CO \quad \text{(IV)}$$

$$C + K_2O \rightarrow 2K + CO \quad [29] \quad \text{(V)}$$

As 40 g powder was taken for carbonization process, 40 g potassium hydroxide (KOH) was measured and it was put in a beaker with 357 mL of water such that the KOH solution's ultimate concentration would be 2 M. Then the

Fig. 1. Preparation of activated orange peel powder.

solution was mixed very well. After that, the orange peel powder was added in the beaker and mixed very well. Then it was left for 24 h at room temperature with a magnetic stirrer. Next day the solution was heated in a Bunsen burner until all the solvent (water) got vaporized. When all the water got vaporized, the solute was taken in a porcelain bowl. Then the solute was kept in a furnace at 700°C for 1 h. After 1 h carbonization process was done and the bowl was taken out from the furnace. In this way the activated carbon from orange peel was produced. Then, the activated carbon obtained from orange peel was taken into a mortar for grinding. After grinding, the activated carbon's mass was calculated and it was 32.51 g. Then, the activated carbon from orange peel was kept in an airtight container for further process so that it could not come in contact with air and absorb moisture. Fig. 1 illustrates the preparation sequence of the activated orange peel powder.

3. Characterization techniques

The properties of natural orange peel and activated orange peel were determined through Fourier-transform infrared spectroscopy (FTIR) and thermogravimetric analysis (TGA).

3.1. Fourier-transform infrared spectroscopy

The FTIR technique can be used to produce an infrared spectrum of an object's absorption or emission. High-resolution spectral data are concurrently collected over a broad spectral range by an FTIR spectrometer. This gives a significant advantage over a dispersive spectrometer, that measures intensity over a constrained spectrum of wavelengths at a time. With the use of FTIR analysis, one can discover unknown compounds, polymer additives, surface contaminants and more. The results of the tests can identify the molecular structure and makeup of a sample [30].

The adsorbents were subjected to FTIR analysis using an IRPrestige-21 spectrophotometer. For measuring absorption spectra, pellets (press disk) were employed. Adsorption may result through complex formation in the ligands present in the adsorbents in addition to electrostatic attraction. A solid, liquid, or gas's vast spectrum range is displayed in high spectral resolution using an FTIR spectrometer.

3.2. Thermogravimetric analysis

In the thermal analysis technique known as TGA, the mass of a sample is tracked over time as the temperature varies. This measurement sheds light on chemical phenomena including chemisorption, thermal breakdown, and solid–gas reactions in addition to physical phenomena like phase transitions, absorption, adsorption, and desorption (e.g., oxidation or reduction). The capacity to correctly estimate a material's strength, stability, and durability has significant implications for modern industry, building, and technology.

A thermogravimetric curve, where mass is plotted as a function of temperature or time, is produced by measuring the sample's mass at regular intervals across this temperature profile. This distinctive curve typically represents thermal decomposition, where high temperatures start to degrade the material. TGA analysis of the adsorbents was performed using a TGA 8000 thermogravimetric analyzer.

3.3. Adsorption experiments

A batch technique was used to examine the adsorption of chromium(III) ions. 20 mL of chromium(III) ions solutions with concentrations of around 20 mg/L were added to 5–40 g/L of adsorbent and shaken at room temperature for 60–120 min at pH 2, 2.8, 3, 4, 6, and 8. The suspension of adsorbent was separated from the solution by filter paper. The concentration of chromium(III) ions remaining in the solution was measured by atomic adsorption spectrometer. Adsorbent dosage, pH, contact time, and other factors were explored as they relate to adsorption, and HCl, buffer solutions, and NaOH were used to modify the pH of the adsorptive solutions. The collected data from this research were utilized to determine the ideal circumstances for achieving the highest levels of chromium(III) removal from tannery wastewater and Buriganga River water. The removal of chromium(III) ions was calculated by given equation:

$$\text{Adsorption}(\%) = \frac{(C_0 - C_e)}{C_0} \times 100 \tag{1}$$

$$q_e = \frac{(C_0 - C_e) \times V}{m} \tag{2}$$

where V (L) is the volume of the solution, m (g) is the mass of the adsorbent, and C_0 (mg/L) and C_e (mg/L) are the starting and final concentrations of chromium, respectively.

3.4. Adsorption isotherm

At constant temperature, the equilibrium relationship between the amount of adsorbate adsorbed on the adsorbent surface and its concentration in the solution was discovered to be the Langmuir isotherm. The Langmuir expression's linear representation is:

$$\frac{C_e}{Q_e} = \frac{C_e}{Q_o} + \frac{1}{(bQ_o)} \tag{3}$$

where C_e is the equilibrium concentration of chromium(III) solution (in mg/L), Q_e is the equilibrium capacity of chromium(III) ions on the adsorbent (in mg/g), Q_o is the adsorbent's capacity for monolayer adsorption, and b is a parameter that is linked to the free energy of adsorption [31].

$$Q_e = (C_o - C_e)\frac{V}{W} \tag{4}$$

where C_e = equilibrium concentration, Q_e = adsorption capacity, V = volume of solution, C_o = initial concentration, W = amount of adsorbent.

The Freundlich isotherm demonstrates that, many layers of adsorbate developed on the adsorbent's surface. This model is based on the presumption that, chromium(III) ions are adsorbed on a heterogeneous surface,

and it is not limited to the production of monomolecular layers. Equation can be used to represent the linear form:

$$\ln Q_e = \ln K_f + \frac{1}{n} C_e \tag{5}$$

The values K_f and $1/n$ represent the adsorption capacity (in mg/g) and intensity, respectively.

3.5. Adsorption kinetics

For the design of adsorption systems, adsorption rate provides essential information. To choose the best circumstances, one must understand the kinetics of pollution removal. To calculate the rate of chromium(III) ion adsorption by natural orange peel (NOP) and activated orange peel (AOP) adsorbent, pseudo-first-order and pseudo-second-order kinetic models were utilized. According to the first-order kinetic model, the metal ion is only restricted to a small portion of the adsorbent's surface. The adsorption rate is inversely correlated with the number of free active sites in this model, which is represented by the following equation [32,33].

$$\log\left(q_e - q\right) = \log q_e - \left(\frac{K_{\text{ads}}}{2.303}\right) t \tag{6}$$

where the so-called first-order adsorption rate constant is given as k_1 (min^{-1}). q_e and q_t are the amounts of material that is adsorbed per unit mass of the adsorbent at equilibrium and in any situation (t). The slope of the line is produced by plotting $\ln(q_e - q_t)$ vs. time (t). The slope is used to derive the values of k_1 and q_e. According to the second-order kinetic model, the chemical reactions that result in the binding of metal ions to the surface via strong bonds that are just as strong as the covalent link dictate the pace of the reaction. Following is the equation that represents the pseudo-second-order model.

$$\frac{t}{q_t} = \frac{1}{k_2 q_e^2} + \frac{t}{q_e} \tag{7}$$

The second-order adsorption rate constant is denoted by the symbol k_2 (g/mg·min). The slope and intercept values for plots of (t/q_t) against (t) are given as $1/q_e$ and $1/k_2 q_e^2$, respectively. R^2 and the computed q_e values are two metrics that may be used to assess how well the kinetic models fit the experimental data. The model that is deemed to be the most compatible is one whose R^2 value is near to 1 and which is close to the computed q_e value of the experimental q_e value.

4. Results and discussions

4.1. Fourier-transform infrared spectroscopy

Through FTIR, it is evident that, at 1,016.30 cm^{-1} C–O stretching, Strong, at 1,356.45 cm^{-1} O–H bending, medium, C=C stretching, medium, at 1,731.63 cm^{-1} C=O stretching, Strong, at 2,916.98 cm^{-1} aliphatic C–H stretching, medium, at 3,271.55 cm^{-1} O–H stretching, broad weak are present in natural orange peel powder and at 700.90 cm^{-1} benzene derivative, at 876.12 cm^{-1}. Oxygen metal bond, at 1,055.47 cm^{-1} C–O stretching, strong, at 1,352.32 cm^{-1} C=O stretching, strong, non-ionic carboxylic group (–COOH, $-COOCH_3$), at 1,447.15 cm^{-1} C–H bending, variable, at 3,125.19 cm^{-1} O–H stretching, broad weak are present in activated orange peel. The predicted peaks are shifted from 1,016.30; 1,356.45; 1,605.89; 2,245.31; 2,916.98 and 3,271.55 cm^{-1} shift to 1,352.32; 1,447.15; 1,743.30; 2,241.95; 2,988.83 and 3,125.19 cm^{-1}, as seen by the strong and sharp peaks at 1,016.75 and 1,354.67 cm^{-1} for NOP and AOP, respectively by this FTIR spectrum [34]. The shift might be brought on by variations in counter ions related to carboxylate and hydroxylate anions. Figs. 2 and 3 below depict the outcomes of FTIR analyses of natural and activated orange peel, respectively.

4.2. Thermogravimetric analysis

From TGA analysis, it is clear that activated orange peel is more resistance to heat than natural orange peel. Because total weight loss from 0°C to 700°C for natural orange peel is 97.48358 whereas delta Y for activated orange peel is 35.89005. The TGA analysis of natural and activated orange peel is shown in Figs. 4 and 5, respectively.

4.3. Adsorption studies

4.3.1. Effect of pH on chromium adsorption

At 298 K, the effect of pH on the adsorption of chromium(III) by natural orange peel and activated orange peel was examined. The concentration and volume of chromium(III) solution were 23.69 mg/L and 20 mL. The impact of pH on the adsorption was investigated in the pH range of 2–8. Because, the real sample solution's pH was often around 3 in nature or higher and the precipitation of metal ions with hydroxide ions typically occurs after pH 7. The maximum adsorption yield was attained at a pH level about 2.8. Additionally, raising of the pH level reduces the adsorption efficiency. It is crucial that no pH

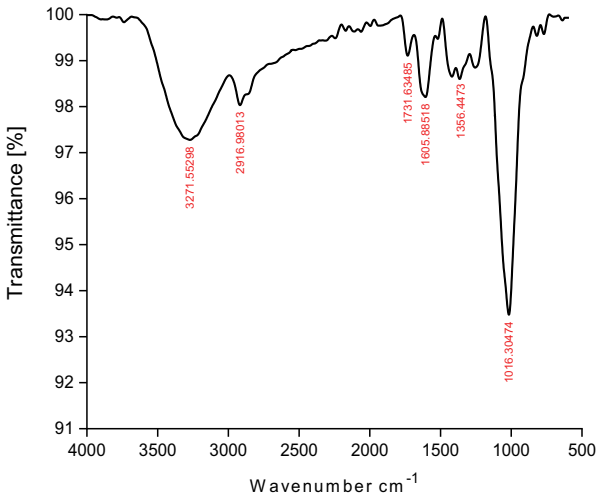

Fig. 2. Fourier-transform infrared spectroscopy spectrum of natural orange peel.

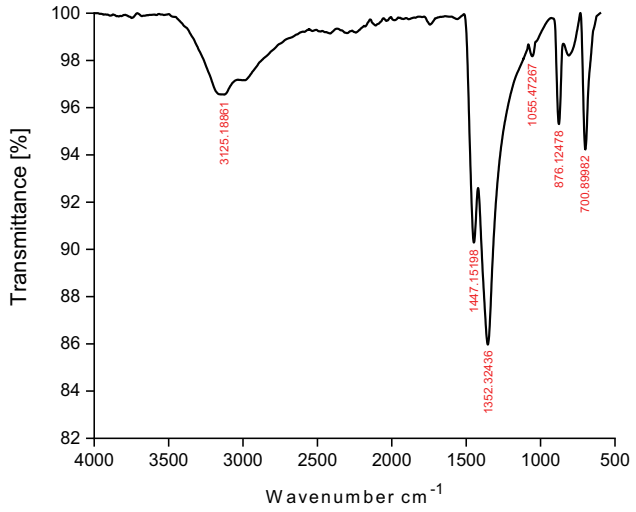

Fig. 3. Fourier-transform infrared spectroscopy spectrum of activated orange peel.

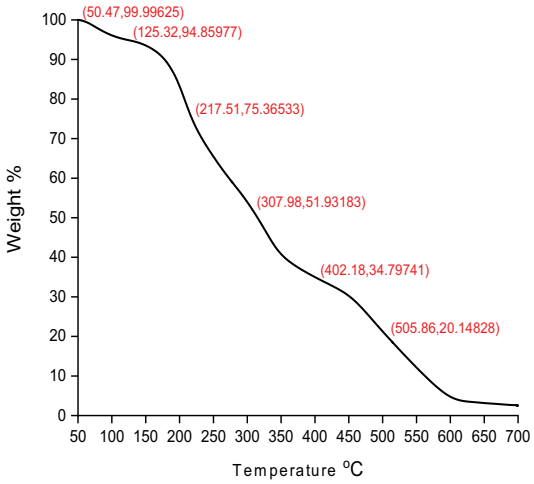

Fig. 4. Thermogravimetric analysis of natural orange peel.

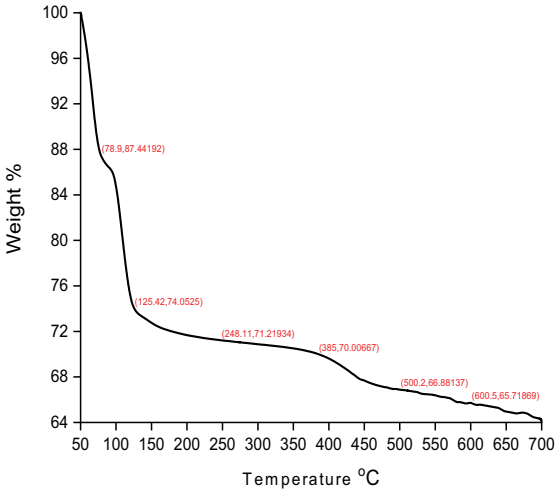

Fig. 5. Thermogravimetric analysis of activated orange peel.

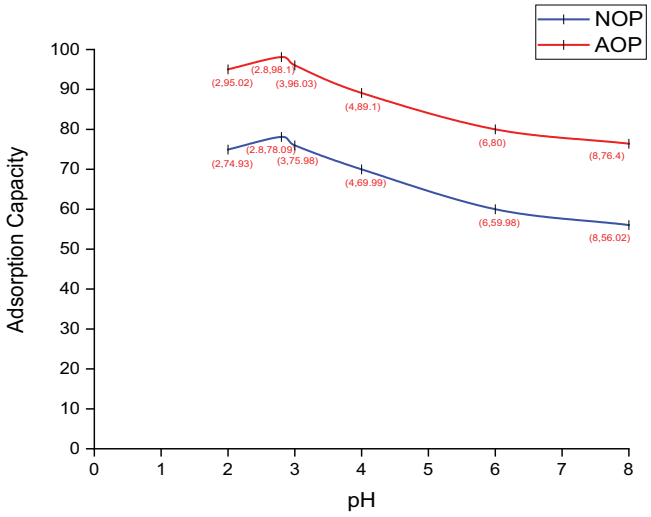

Fig. 6. Effect of pH on natural orange peel and activated orange peel.

correction is required because the produced solution was roughly pH 2.8 which is acidic. These findings indicate that different chromium species in the solution have varying affinities for the carbon surface, and that the affinities of the chromium(III) ions are strongly influenced by the pH of the solution, which is why maximal adsorption (at pH 2–3.2) occurs. Because chromium(III) is oxidized in aqueous solution to CrO_4^{2-}, which is negatively charged and can be adsorbable via protonated groups on the adsorbent's surface at low pH levels. Adsorption tests were carried out at various pH levels 2.0, 2.8, 3, 4, 6, 8.

At a pH range of 2.0–2.8, the removal efficiency rose for NOP from 74.93% to 78.09% and for AOP from 95.02% to 98.10%, respectively. At a pH range of 2.8–8, the removal efficiency dropped. The rise in percentage adsorption and uptake at lower pH might both be explained by the protonation properties of the adsorbent. The negative charge at the surface of internal pores was neutralized by low pH values or higher hydrogen ion concentrations, which also stimulated the growth of new adsorption sites and gave anionic chromium(III) complex a positive charge to cling to the surface. The H^+ ions were further neutralized by the surface's negative charge, which fostered the growth of a positively charged surface, and by the encirclement of more H^+ ions. The solution's ultimate pH was continuously higher than its original pH. The pH of the solution rose as a consequence of the reduction in the amount of H^+ ions present. The investigation revealed that the optimal pH for both NOP and AOP to remove the highest amount of Cr(III) ion was 2.8. Fig. 6 demonstrates the impact of pH on both natural orange peel and activated orange peel.

4.3.2. *Effect of adsorbent dose on chromium adsorption*

The quantity of adsorbent is a key factor in determining the metal removal potential at any concentration at any component. To examine the effect of NOP and AOP amounts on the chromium adsorption, 20 mL of a

20.65 mg/L chromium(III) solution with 5–40 g/L of adsorbent quantity were employed. As the quantity of adsorbents rose, the removal of chromium(III) increased as well. It was discovered that, at 8 g/L of NOP and AOP adsorbent generated the highest adsorption efficiency. Additionally, there was no discernible difference in the rise in adsorption efficiency when the adsorbent concentration was higher than 8 g/L. The trials at this point were conducted with a pH of 2.8 and varying adsorbent dosages (5, 8, 10, 20, 30 and 40 g/1,000 mL). The following Fig. 7 demonstrates that the rise in removal efficiency with a rise in adsorbent dosage may be due to the availability of freer surfaces, which increased the number of adsorbate molecules that might adsorb. The investigation revealed that the optimal amount of adsorbent dose for both NOP and AOP to remove the highest amount of Cr(III) ion was 8 g/L (Fig. 7).

4.3.3. Effect of contact time on chromium adsorption

In order to ascertain the equilibrium, contact time, experiments were done for a total of 2 h. According to the experimental findings, percentage of adsorption increased with longer contact times up to 60 min before reaching a stationary phase. Additionally, the smooth and continuous graphs between timings and percentage adsorption suggested a potential monolayer adsorption of chromium(III) on the surface of the adsorbent. With the exception of contact duration, all of the other variables in this stage remained constant, including temperature (room temperature), adsorbent dose (8 g/L), pH (2.8), starting chromium concentration (20.80 mg/L), and agitation speed (150 rpm). After 60 min, the adsorption phase reached equilibrium.

There are a lot of empty surface sites accessible for adsorption in the early stages of sorption. Because of the repelling interactions between the molecules of the adsorbate on the solid surface and those in the bulk phase, it takes a long time for the remaining empty surface sites to be filled. The metal ions are also taken up by the mesopores, that are nearly saturated at the beginning of adsorption. As a result, as time goes on, less energy is required to drive mass transfer between the solid phase and the bulk liquid phase. Moreover, there is considerably more resistance to overcome since the metal ions must penetrate the pores at a deeper and deeper depth [35]. The adsorption during the later phase slows down as a result. Since adsorption is a process that is time-dependent, it is essential to understand the adsorption rate while constructing a process. The influence of the contact time of chromium(III) ions on adsorption with NOP and AOP was investigated at various chromium ion starting concentrations in order to determine the equilibrium time to most efficiently remove chromium(III) ions and the kinetics of the adsorption process. Under active experimental circumstances, equilibrium is established in less than 60 min. After 60 min of contact, the increase in adsorption efficiency does not seem to be very noticeable. Because of this, the equilibrium time was established as the first 60 min of interaction. This outcome demonstrates that a longer contact is not feasible because, in equilibrium, the adsorbent surface gets saturated with chromium(III) ions. Therefore, the investigation revealed that the optimal contact time for both NOP and AOP to remove the highest amount of Cr(III) ion was 60 min. Fig. 8 depicts the influence of contact time on both natural orange peel and activated orange peel.

4.4. Adsorption isotherms

The Langmuir isotherm for natural orange peel (NOP) and activated orange peel (AOP) is also presented in Figs. 9 and 10, respectively.

Since the R^2 value is near to 1, both models accurately describe the system, but the Freundlich isotherm model fits the data better which is shown in the Table 1.

The experimental data's agreement with the Freundlich isotherm model leads to the conclusion that the adsorption occurs on a heterogeneous solid surface. According to Guiza [36], the original orange peel was used to execute the Freundlich isotherm model on copper adsorption. On the other hand, Marin et al. [37] observed that the adsorption

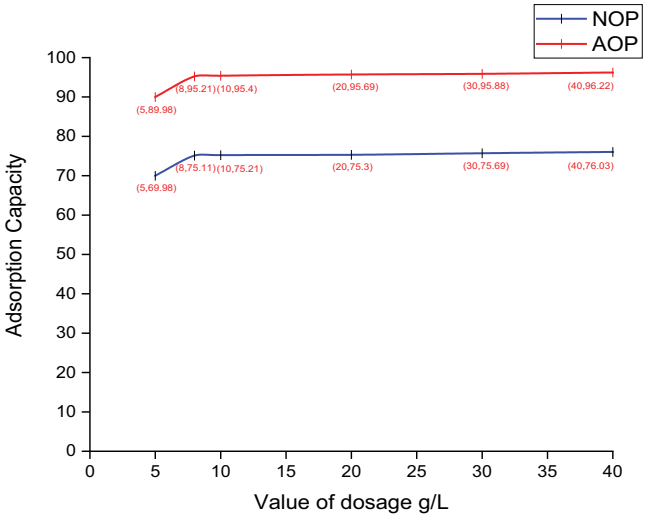

Fig. 7. Effect of adsorbent dose on natural orange peel and activated orange peel.

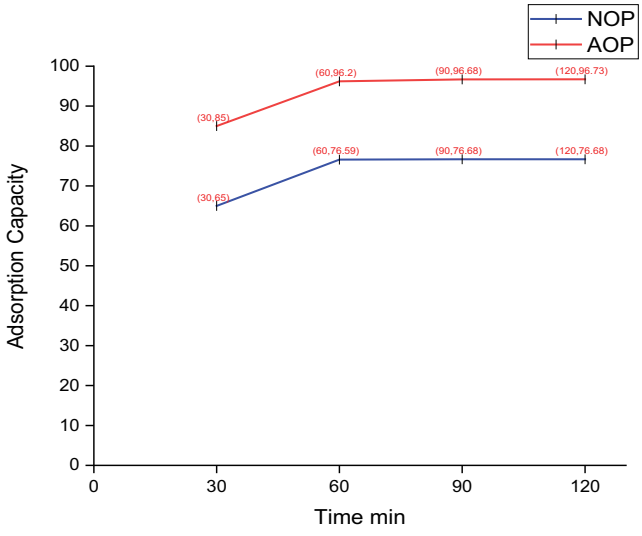

Fig. 8. Effect of contact time on natural orange peel and activated orange peel.

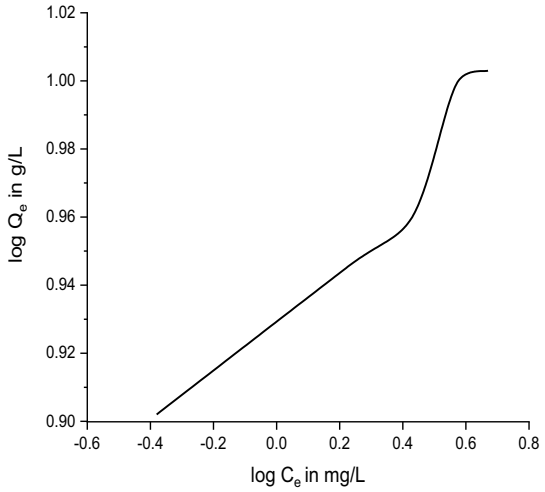

Fig. 9. Langmuir isotherm for natural orange peel.

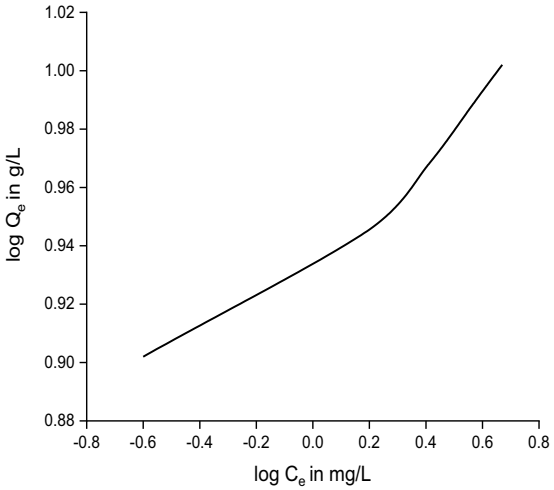

Fig. 10. Langmuir isotherm for activated orange peel.

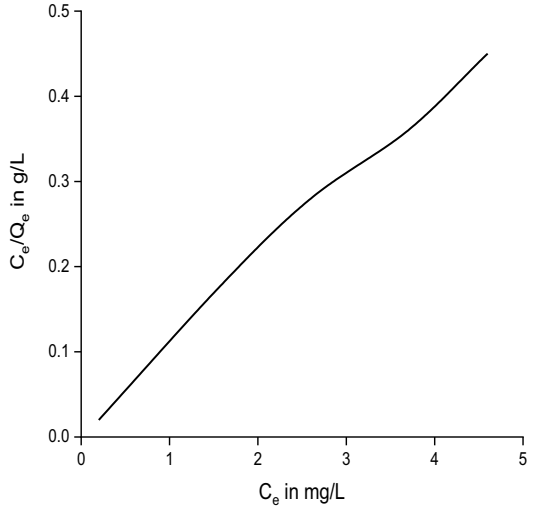

Fig. 11. Freundlich isotherm for natural orange peel.

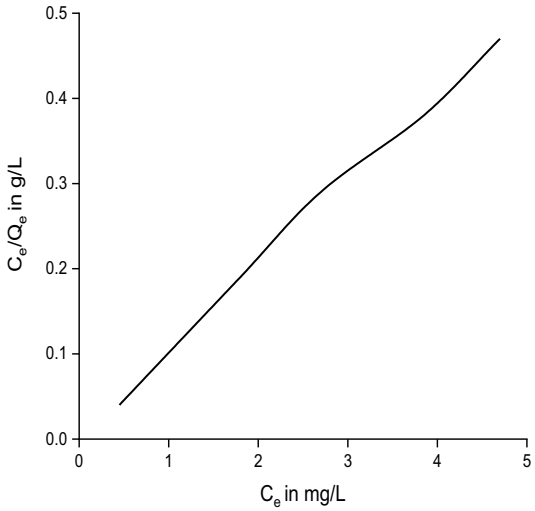

Fig. 12. Freundlich isotherm for activated orange peel.

Table 1
Observation of adsorption constants for natural orange peel and activated orange peel at the room temperature for different isotherm mode

	Langmuir isotherm model			Freundlich isotherm model		
	Q_m	K_L	R^2	N	K_f	R^2
Natural orange peel	0.099	20.66	0.93139	1.05	2.38	0.99355
Activated orange peel	0.095	6.85	0.95395	1.10	2.62	0.9958

Table 2
Kinetic parameters for the adsorption of chromium(III) for natural orange peel and activated orange peel at 298 K

	Pseudo-first-order		Pseudo-second-order	
	k_1	R^2	k_2	R^2
Natural orange peel	0.062953	0.93139	0.501	0.99355
Activated orange peel	0.071679	0.95395	0.792	0.9958

capacity of Cr(III) ions utilizing orange trash was higher than that of activated with formaldehyde, methanol, and acetic acid, and this adsorption was described as a Langmuir isothermic model. Another research used the Langmuir isotherm model to easily adsorb Cr(III) ions from orange peel that had been formaldehyde-activated [2].

4.5. Adsorption kinetics

The second-order kinetic model can accommodate the adsorption of chromium(III) ions because of correlation coefficients obtained from the kinetic equations are higher for

Table 3
Determination of the adsorption of chromium(III) from chrome liquor after chrome tanning by natural orange peel powder

Adsorption of chromium(III) from chrome liquor after chrome tanning by natural orange peel powder		
Chromium(III) concentration before adsorption	122.40 mg/L	
Chromium(III) concentration after adsorption	28.16 mg/L	Removal efficiency = 76.99%
Concentration of adsorbed chromium(III)	94.24 mg/L	

Table 4
Determination of the adsorption of chromium(III) from chrome liquor after chrome tanning by activated orange peel powder

Adsorption of chromium(III) from chrome liquor after chrome tanning by activated orange peel powder		
Chromium(III) concentration before adsorption	122.40 mg/L	
Chromium(III) concentration after adsorption	4.89 mg/L	Removal efficiency = 96.00%
Concentration of adsorbed chromium(III)	117.51 mg/L	

Table 5
Determination of the adsorption of chromium(III) from Buriganga River water by natural orange peel powder

Adsorption of chromium(III) from Buriganga River water by natural orange peel powder		
Chromium(III) concentration before adsorption	7.37 mg/L	
Chromium(III) concentration after adsorption	1.69 mg/L	Removal efficiency = 77.07%
Concentration of adsorbed chromium(III)	5.68 mg/L	

the quadratic equation. Furthermore, the actual ($q_{e,\exp}$) values and the theoretical q_e values generated from the model equations are very close. Also, the second-order kinetic model gets close to a R^2 value of 1 which is seen in the Table 2.

This shows that the second-order kinetic model more closely matches the experimental data. These results suggest that the adsorption of chromium(III) ions onto the NOP and AOP adsorbent is a second-order process.

4.6. Determination of adsorption of chromium(III) from tannery chrome liquor and Buriganga River water at ideal pH, contact time, temperature and amount of dosage

Chrome liquor was collected after chrome tanning from apex tannery situated in Hemayetpur, Savar. Water from Buriganga River was also collected. Then, the concentration of chromium(III) in both samples was measured by atomic absorption spectroscopy (AAS) machine. After that, both the samples were treated by NOP and AOP at pH 2.8 and room temperature. The contact time was 60 min and amount of dosage was 8 g/L. After 60 min of shaking, the solution was filtered and the amount of chromium(III) that did not adsorb was measured by AAS machine. Tables 3–6 display the results of the adsorption of chromium(III) from tannery chrome liquor and Buringanga river water at optimal parameters.

Table 6
Determination of the adsorption of chromium(III) from Buriganga River water by activated orange peel powder

Adsorption of chromium(III) from Buriganga River water by activated orange peel powder		
Chromium(III) concentration before adsorption	7.37 mg/L	
Chromium(III) concentration after adsorption	0.30 mg/L	Removal efficiency = 95.93%
Concentration of adsorbed chromium(III)	7.07 mg/L	

5. Conclusion

The findings of the experiment indicate that natural orange peel and activated orange peel are excellent alternatives for removing chromium(III) from aqueous solutions as the adsorbents are inexpensive and ecofriendly compared to the other existing methods. The research's results are just as impressive as those of other notable studies [38–44]. Particle sizes, pH, particle sizes, contact time, adsorbent dosage and initial chromium content all had an impact on the adsorption of chromium(III). It was discovered that the optimal conditions for Cr(III) absorption by NOP and AOP are pH 2.8, 60 min, and 8 g of adsorbent per 1,000 mL. In this optimal condition the adsorption capacity for NOP and AOP to remove chromium(III) from waste water was 77% and 96%, respectively. The subsequent appearance of chromium(III) adsorption was seen after Freundlich isotherms. The study's kinetic analysis demonstrated that the pseudo-second-order kinetic model could adequately represent the adsorption of chromium(III) ions onto NOP and AOP. According to the findings of this study, natural and activated orange peel are suitable adsorbents for removing chromium from tannery wastewater since they are readily accessible, inexpensive, and ecologically acceptable.

Acknowledgement

For providing the facilities needed for this investigation, the authors are grateful to the Institute of Leather Engineering and Technology, University of Dhaka.

References

[1] S. Kumaraguru, T.P. Sastry, C. Rose, Hydrolysis of tannery fleshing using pancreatic enzymes: a biotechnological tool for solid waste management, J. Am. Leather Chem. Assoc., 93 (1998) 32–39.

[2] Y. Arslan, E. Kendüzler, B. Kabak, K. Demir, F. Tomul, Determination of adsorption characteristics of orange peel activated with potassium carbonate for chromium(III) removal, J. Turk. Chem. Soc., 4 (2017) 51–64.
[3] Md. S.S. Shibli, Md. T. Islam, In Bangladesh, Tanneries in Trouble, The Asia Foundation, 465 California St., 9th Floor, San Francisco, CA 94104, 2020. Available at: https://asiafoundation.org/2020/05/27/in-bangladesh-tanneries-in-trouble/
[4] Md. R. Awual, Novel ligand functionalized composite material for efficient copper(II) capturing from wastewater sample, Composites, Part B, 172 (2019) 387–396.
[5] Md. R. Awual, Mesoporous composite material for efficient lead(II) detection and removal from aqueous media, J. Environ. Chem. Eng., 7 (2019) 103124, doi: 10.1016/j.jece.2019.103124.
[6] Md. R. Awual, Novel conjugated hybrid material for efficient lead(II) capturing from contaminated wastewater, Mater. Sci. Eng., C, 101 (2019) 686–695.
[7] Md. R. Awual, Md. M. Hasan, A. Islam, M.M. Rahman, A.M. Asiri, Md. A. Khaleque, Md. C. Sheikh, Offering an innovative composited material for effective lead(II) monitoring and removal from polluted water, J. Cleaner Prod., 231 (2019) 214–223.
[8] Md. R. Awual, T. Yaita, T. Kobayashi, H. Shiwaku, S. Suzuki, Improving cesium removal to clean-up the contaminated water using modified conjugate material, J. Environ. Chem. Eng., 8 (2020) 103684, doi: 10.1016/j.jece.2020.103684.
[9] Md. R. Awual, Efficient phosphate removal from water for controlling eutrophication using novel composite adsorbent, J. Cleaner Prod., 228 (2019) 1311–1319.
[10] Md. R. Awual, Md. M. Hasan, A. Shahat, Mu. Naushad, H. Shiwaku, T. Yaita, Investigation of ligand immobilized nano-composite adsorbent for efficient cerium(III) detection and recovery, Chem. Eng. J., 265 (2015) 210–218.
[11] Md. R. Awual, Md. M. Hasan, A.M. Asiri, M.M. Rahman, Novel optical composite material for efficient vanadium(III) capturing from wastewater, J. Mol. Liq., 283 (2019) 704–712.
[12] Md. R. Awual, Md. M. Hasan, Md. A. Khaleque, Md. C. Sheikh, Treatment of copper(II) containing wastewater by a newly developed ligand based facial conjugate materials, Chem. Eng. J., 288 (2016) 368–376.
[13] Md. R. Awual, Md. M. Hasan, M.M. Rahman, A.M. Asiri, Novel composite material for selective copper(II) detection and removal from aqueous media, J. Mol. Liq., 283 (2019) 772–780.
[14] Md. R. Awual, A novel facial composite adsorbent for enhanced copper(II) detection and removal from wastewater, Chem. Eng. J., 266 (2015) 368–375.
[15] M.M. Kabir, Mst. M. Akter, S. Khandaker, B.H. Gilroyed, Md. Didar-ul-Alam, M. Hakim, Md. Rabiul Awual, Highly effective agro-waste based functional green adsorbents for toxic chromium(VI) ion removal from wastewater, J. Mol. Liq., 347 (2022) 118327, doi: 10.1016/j.molliq.2021.118327.
[16] Md. A. Islam, M.J. Angove, D.W. Morton, B.K. Pramanik, Md. R. Awual, A mechanistic approach of chromium(VI) adsorption onto manganese oxides and boehmite, J. Environ. Chem. Eng., 8 (2020) 103515, doi: 10.1016/j.jece.2019.103515.
[17] S.P. Mahajan, Pollution Control in Process Industries, Tata McGraw Hill Publishing Company, 1985. Available at: https://books.google.com.bd/books/about/Pollution_Control_In_Process_Industries.html?id=HRYjBpsmzXMC&redir_esc=y
[18] F. Gode, E. Pehlivan, Removal of chromium(III) from aqueous solutions using Lewatit S 100: the effect of pH, time, metal concentration and temperature, J. Hazard. Mater., 136 (2006) 330–337.
[19] F.J. Alguacil, I. Garcia-Diaz, F. Lopez, The removal of chromium(III) from aqueous solution by ion exchange on Amberlite 200 resin: batch and continuous ion exchange modelling, Desal. Water Treat., 45 (2012) 55–60.
[20] N. Kabay, N. Gizli, M. Demircioğlu, M. Yuksel, A. Jyo, K. Yamabe, T. Shuto, Cr(III) removal by macroreticular chelating ion exchange resins, Chem. Eng. Commun., 190 (2010) 813–822.
[21] M. Keshavarz, R. Foroutan, F. Papari, L. Bulgariu, H. Esmaeili, Synthesis of CaO/Fe_2O_3 nanocomposite as an efficient nanoadsorbent for the treatment of wastewater containing Cr(III), Sep. Sci. Technol., 56 (2020) 1328–1341.
[22] B.H. Hintermeyer, N.A. Lacour, A. Perez Padilla, E.L. Tavani, Separation of the chromium(III) present in a tanning wastewater by means of precipitation, reverse osmosis and adsorption, Latin Am. Appl. Res., 38 (2008) 63–71.
[23] E. Abbasi-Garravand, C.N. Mulligan, Using micellar enhanced ultrafiltration and reduction techniques for removal of Cr(VI) and Cr(III) from water, Sep. Purif. Technol., 132 (2014) 505–512.
[24] Y. Zhang, X. Xu, C. Yue, L. Song, Y. Lv, F. Liu, A. Li, Insight into the efficient co-removal of Cr(VI) and Cr(III) by positively charged UiO-66-NH_2 decorated ultrafiltration membrane, Chem. Eng. J., 404 (2021) 126546, doi: 10.1016/j.cej.2020.126546.
[25] T. Mohammadi, A. Moheb, M. Sadrzadeh, A. Razmi, Modeling of metal ion removal from wastewater by electrodialysis, Sep. Purif. Technol., 41 (2005) 73–82.
[26] Y. Liu, X. Ke, X. Wu, C. Ke, R. Chen, X. Chen, X. Zheng, Y. Jin, B. Van der Bruggen, Simultaneous removal of trivalent chromium and hexavalent chromium from soil using a modified bipolar membrane electrodialysis system, Environ. Sci. Technol., 54 (2020) 13304–13313.
[27] I.S. Bădescu, D. Bulgariu, I. Ahmad, L. Bulgariu, Valorisation possibilities of exhausted biosorbents loaded with metal ions – a review, J. Environ. Manage., 224 (2018) 288–297.
[28] G. El Mouhri, M. Merzouki, H. Belhassan, Y. Miyah, H. Amakdouf, R. Elmountassir, A. Lahrichi, Continuous adsorption modeling and fixed bed column studies: adsorption of tannery wastewater pollutants using beach sand, J. Chem., 2020 (2020) 7613484, doi: 10.1155/2020/7613484.
[29] K. Subramani, N. Sudhan, M. Karnan, M. Sathish, Orange peel derived activated carbon for fabrication of high-energy and high-rate supercapacitors, ChemistrySelect, 2 (2017) 11384–11392.
[30] J. Mathias, How Does FTIR Analysis Work?, Innovatech Labs, LLC, 13805 1st Ave N, Ste 100, Plymouth, MN 55441, 888-740-5227, 2015. Available at: https://www.innovatechlabs.com/newsroom/672/stuff-works-ftir-analysis/
[31] N. Feng, X. Guo, S. Liang, Adsorption study of copper(II) by chemically modified orange peel, J. Hazard. Mater., 162 (2009) 616–645.
[32] J. Febrianto, A.N. Kosasih, J. Sunarso, Y.-H. Ju, N. Indraswati, S. Ismadji, Equilibrium and kinetic studies in adsorption of heavy metals using biosorbent: a summary of recent studies, J. Hazard. Mater., 162 (2009) 616–645.
[33] M. Basu, A.K. Guha, L. Ray, Adsorption of lead on cucumber peel, J. Cleaner Prod., 151 (2017) 603–615.
[34] E. Bernard, A. Jimoh, Adsorption of Pb, Fe, Cu, and Zn from industrial electroplating wastewater by orange peel activated carbon, Int. J. Eng. Appl. Sci., 4 (2013) 95–103.
[35] S. Srivastava, I.S. Thakur, Isolation and process parameter optimization of *Aspergillus* sp. for removal of chromium from tannery effluent, Bioresour. Technol., 97 (2006) 1167–1173.
[36] S. Guiza, Biosorption of heavy metal from aqueous solution using cellulosic waste orange peel, Ecol. Eng., 99 (2017) 134–140.
[37] A.B. Pérez Marín, J.F. Ortuño, M.I. Aguilar, V.F. Meseguer, J. Sáez, M. Lloréns, Use of chemical modification to determine the binding of Cd(II), Zn(II) and Cr(III) ions by orange waste, Biochem. Eng. J, 53 (2010) 2–6.
[38] Md. R. Awual, A facile composite material for enhanced cadmium(II) ion capturing from wastewater, J. Environ. Chem. Eng., 7 (2019) 103378, doi: 10.1016/j.jece.2019.103378.
[39] Mu. Naushad, A.A. Alqadami, A.A. Al-Kahtani, T. Ahamad, Md. R. Awual, T. Tatarchuk, Adsorption of textile dye using para-aminobenzoic acid modified activated carbon: kinetic and equilibrium studies, J. Mol. Liq., 296 (2019) 112075, doi: 10.1016/j.molliq.2019.112075.
[40] S. Khandaker, M.F. Chowdhury, Md. R. Awual, A. Islam, T. Kuba, Efficient cesium encapsulation from contaminated water by cellulosic biomass based activated wood charcoal, Chemosphere, 262 (2021) 127801, doi: 10.1016/j.chemosphere.2020.127801.

[41] A. Islam, S.H. Teo, Md. R. Awual, Y.H. Taufiq-Yap, Assessment of clean H_2 energy production from water using novel silicon photocatalyst, J. Cleaner Prod., 244 (2020) 118805, doi: 10.1016/j.jclepro.2019.118805.
[42] Md. N. Hasan, M.A. Shenashen, Md. M. Hasan, H. Znad, Md. R. Awual, Assessing of cesium removal from wastewater using functionalized wood cellulosic adsorbent, Chemosphere, 270 (2021) 128668, doi: 10.1016/j.chemosphere.2020.128668.
[43] Md. B. Yeamin, Md. M. Islam, A.-N. Chowdhury, Md. R. Awual, Efficient encapsulation of toxic dyes from wastewater using several biodegradable natural polymers and their composites, J. Cleaner Prod., 291 (2021) 125920, doi: 10.1016/j.jclepro.2021.125920.
[44] K.T. Kubra, Md. S. Salman, Md. N. Hasan, A. Islam, S.H. Teo, Md. M. Hasan, Md. C. Sheikh, Md. R. Awual, Sustainable detection and capturing of cerium(III) using ligand embedded solid-state conjugate adsorbent, J. Mol. Liq., 338 (2021) 116667, doi: 10.1016/j.molliq.2021.116667.